EMI R&D PROJECT FINAL REPORT

All the following mandatory information needs to be provided.

Project Title:	IMPROVING DUST TRANSPORT MODELS USING AEOLUS DATA ASSIMILATION (DUSTAR)
Computer Project Account:	spgramir
Start Year - End Year :	2023 - 2025
Principal Investigator(s)	Dr. Vassilis Amiridis
Affiliation/Address:	National Observatory of Athens (NOA) Metaxa & Vasileos Pavlou, 145 76, Athens, Greece
Other Researchers (Name/Affiliation):	• Anna Gialitaki (NOA) • Eleni Drakaki (NOA) • Thanasis Georgiou (NOA) • Alexandra Tsekeri (NOA)

The following should cover the entire project duration.

Summary of project objectives

(10 lines max)

ESA's wind mission Aeolus carried ALADIN, the first space-based Doppler wind lidar, aimed at improving numerical weather prediction through wind profile measurements. Aeolus also provided profiles of cloud and aerosol optical properties. This project developed the tools and observation operators to assimilate both L2 Aeolus products, lidar extinction (L2A) and HLOS winds (L2B), into an atmospheric composition model, and studied how each constrains the dust field. The model is WRF-Chem (GOCART scheme for desert dust and sea salt), run as a 30-member EnKF (NCAR DART) ensemble over a North Africa and North Atlantic domain. The study period is September 2022, overlapping the ESA-ASKOS and NASA-CPEX-CV campaigns over Cabo Verde. Results show that the two products act through different mechanisms, with extinction constraining the aerosol field directly and winds affecting dust indirectly through transport. This indicates complementary information content and motivates further atmospheric lidar assimilation, particularly given the launch of EarthCARE and its ATLID instrument.

Summary of problems encountered

(If you encountered any problems of a more technical nature, please describe them here.)

We did not encounter any significant technical issues on the HPC. At the time of writing the original project proposal, we underestimated the development effort needed for the assimilation system and operators, which led to an underutilisation of allocated resources for the first half of the project. Utilisation improved during the later parts of the project, at which point the developments were mostly finished and we could focus on the scientific experiments.

Due to the 30 running jobs limit implemented, we reduced our ensemble size from the planned 32 members to 30 actual members, which in turn reduced perceived wall time to half because all members of the ensemble would execute in parallel. We don’t believe this had any perceptible impact on the results.

Experience with the EMI R&D Project framework

(Please let us know about your experience with administrative aspects like the application procedure, progress reporting etc.)

Our experience with the EMI R&D project framework has been very positive. The application and reporting requirements are reasonable, well defined and not a significant administrative burden on the project team. The allocated resources are significant, and the HPC environment is very convenient to work in, in terms of software availability, storage space and queue waiting times. The public list of projects and reports is a good source of inspiration.

Summary of results

(This section should comprise up to 10 pages, reflecting the complexity and duration of the project, and can be replaced by a short summary plus an existing scientific report on the project.)

Introduction

Atmospheric aerosols are a major source of uncertainty in weather and climate prediction, and mineral dust is among the most important species both for its large mass loading in specific regions and for its direct and indirect effects on radiation and clouds. Operational systems typically constrain aerosols through Aerosol Optical Depth (AOD), a columnar quantity that corrects the total load but provides little information on the vertical distribution, which is exactly what matters for radiative and cloud interactions and for long-range transport. Space-based atmospheric lidars address this gap directly. By measuring backscatter and extinction throughout the column, they constrain the vertical structure of the aerosol field rather than only its integral.

ESA's Aeolus mission offers a distinctive opportunity in this context, because it provides both a wind product (HLOS line-of-sight winds, L2B) and an aerosol product (lidar extinction, L2A) from the same platform. This allows the two assimilation pathways to be studied within a single modelling framework: extinction, which constrains the aerosol field directly, and winds, which act on dust indirectly through the dynamical fields that transport and emit it. The objective of this project was to develop the tools and observation operators required to assimilate both products into a coupled atmospheric composition model, and to characterise how each constrains the dust field.

To this end we built a cycling assimilation system based on WRF-Chem coupled with the NCAR-DART ensemble framework, run over a domain covering North Africa and the North Atlantic during September 2022. This period overlaps the ESA-ASKOS and NASA-CPEX-CV field campaigns over the Cabo Verde region, providing independent reference measurements for evaluation. Three configurations were run, a control without assimilation and two assimilation experiments using the L2A and L2B products respectively, allowing the impact of each product to be isolated. The system and its data flow are summarised in Figure 1.

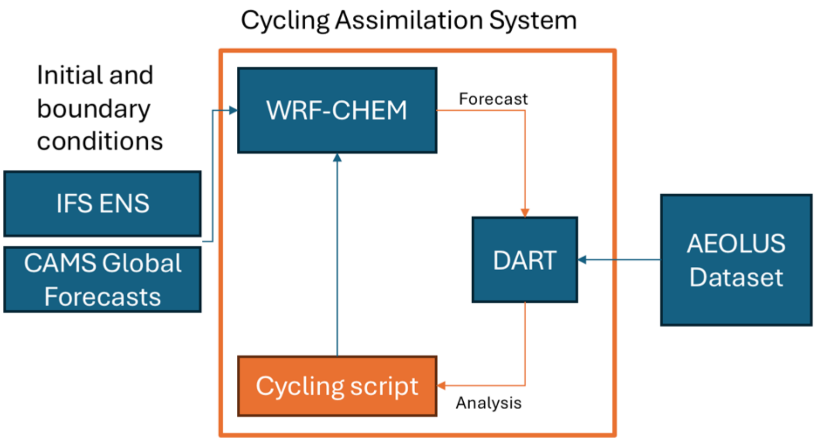

Figure 1: Overview of the cycling assimilation system, showing the main data flows. New developments are marked with orange.

System configuration

The system couples WRF-Chem v4.7.1 with the NCAR Data Assimilation Research Testbed (DART), using the Ensemble Adjustment Kalman Filter (EAKF). The model is configured at 27 km horizontal resolution with 45 vertical levels, reaching 50 hPa at the top, and uses the Morrison two-moment cloud microphysics scheme, the RRTMG radiation scheme, the MYJ planetary boundary layer scheme, and the five-size-bin GOCART desert dust scheme with AFWA emissions. Of the available aerosol species, only desert dust and sea salt are simulated, being the species relevant over the study region. A 30-member ensemble is advanced forward in time, initialised and forced by the ECMWF IFS-ENS for the meteorological fields and by CAMS global forecasts for the aerosol fields; each member carries its own meteorological and emission state, so that the ensemble spread at any analysis time expresses the combined uncertainty in the meteorological and dust fields. The domain covers North Africa and the North Atlantic, over the period of September 2022. Three configurations were run under otherwise identical settings: a control without assimilation (NoDA), assimilation of the Aeolus L2A extinction product, and assimilation of the Aeolus L2B HLOS wind product.

Cycling and the assimilation window

The system advances the ensemble forward, halts at fixed analysis times to assimilate the available observations, updates each member, and restarts it from its analysis, repeating the loop across the period. The model was cycled every 3 h, with observations assimilated in a ±1 h window centred on each analysis time. Coverage is therefore opportunistic with overpasses falling within the window ingested at the cycle's analysis time, while cycles with no overpass in the window receive no observations and the model is simply carried forward from the previous forecast. The choice of horizontal resolution is tied to the length of the assimilation window. Because all observations within a window are compared against the model state at the single analysis time, an advected feature that crosses one or more grid cells during the window introduces a representativeness mismatch, which is absorbed into the observation error budget. The chosen relevant timescale is the cell-crossing time, $\Delta x/U$, the interval an advected feature (dust in this case) takes to traverse a grid cell of width Δx at wind speed U. To ground this in the transport conditions of the region, the horizontal wind speed was averaged over the 850 to 550 hPa layer, which contains the bulk of the Saharan Air Layer, over a North Africa and Mediterranean box restricted to cells with appreciable coarse-mode dust load. The resulting distribution (Figure 2) has a median near 8.5 m/s and a 90th percentile near 14 m/s. At 27 km, these speeds hold feature displacement to roughly two grid cells at the median and four at the 90th percentile over the window, keeping representativeness error bounded while retaining usable spatial detail. A finer grid would force a proportionally shorter window and raise the computational cost of each ensemble integration, while a coarser one would sacrifice spatial detail that the analysis needs.

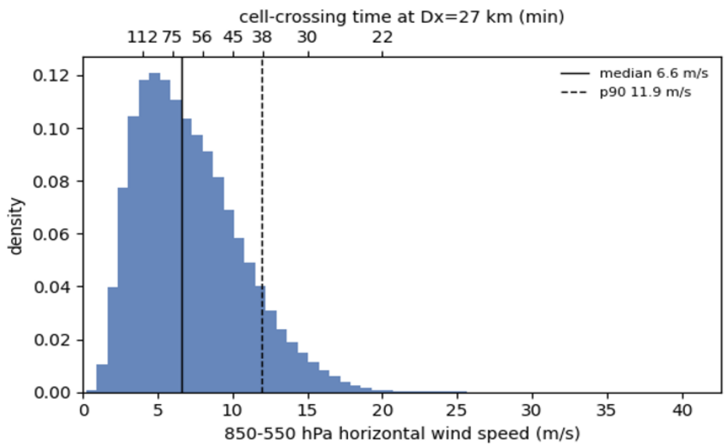

Figure 2: Distribution of horizontal wind speed averaged over the 850 to 550 hPa layer, within the SAL region defined by the geographic box and the coarse-mode dust AOD condition. The upper axis converts wind speed to the cell-crossing time at 27 km grid spacing.

Observations and quality control

The Aeolus L2A product provides profiles of particulate extinction at 355 nm. Of the three extinction retrievals it contains, produced by different algorithms, the AEL-PRO retrieval was assimilated. The AEL-PRO product shares its basic algorithm with the EarthCARE extinction retrieval, giving the operator developed here forward heritage toward ATLID. The L2B product provides horizontal line-of-sight (HLOS) wind profiles. Prior to assimilation, observations were screened by a quality-control mask that removed cloud-contaminated and otherwise unreliable retrievals. Cloud screening is particularly consequential for the extinction product over this region, since it preferentially removes observations within the Saharan Air Layer, where the dust signal, and therefore the constraining power of the observations, is strongest. The effect of the assimilation at the level of a single overpass, from raw observations through the quality-control mask to the resulting analysis increment, is illustrated in Figure 3. The exact masking steps for extinction (L2A) are:

- Keep only bins classified as stratospheric or tropospheric aerosols (`ael_pro_opt_properties/measurement_ael_pro_optical_properties/height_bin_ael_pro_optical_properties/classification`)
- Keep only bins without any indicated quality issues (`measurement_ael_pro_pcd/quality_index`). Any bins with bits #0-3 and #5 set are dropped. Bit #4 indicates 'maximum iterations reached (measurement level)' but it was set very often and was therefore ignored to preserve some data density.

And for L2B observations:

- Keep only Rayleigh-Clear and Mie-Cloudy observations
- Remove any observations marked as invalid (`windresult/validity_flag`)

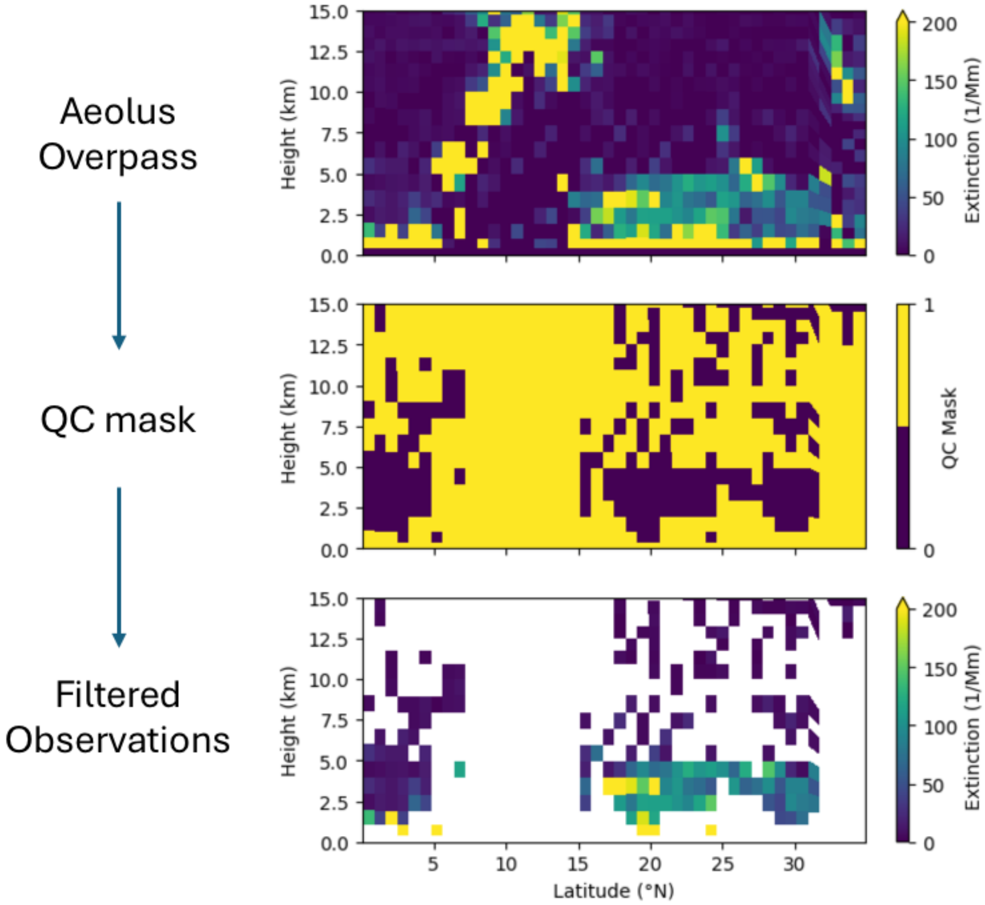

Figure 3: An indicative Aeolus L2A overpass, the corresponding quality control (QC) mask and the final observations used for assimilation. Note the filtered clouds at the top left of the scene.

As far as the observation error is concerned, for L2A Extinction it was set to 30% of the extinction value with a minimum of $10\times^{-5}$ m^{-1}, determined empirically through a short O-B analysis of a model free run. For L2B HLOS Wind observations, the error for Rayleigh observations was set to 4.5 m/s and for Mie observations to 2.5 m/s, according to literature[1].

Ensemble spread

Ensemble spread in the meteorological state is inherited from the ECMWF IFS-ENS, each member being initialised and forced by a distinct IFS-ENS realisation. This meteorological spread also provides a baseline spread in the dust field itself. Because each member transports the aerosol along a slightly different wind field, an initially shared dust distribution diverges between members through differential transport alone.

Spread in the aerosol state is then reinforced by perturbations acting directly on the dust and sea-salt fields. The first component seeds placement uncertainty by assigning each member a small fixed horizontal offset of the global aerosol initial and boundary fields, of the order of one degree and applied identically to that member's initial condition and to all of its boundary updates. Because a spatial shift perturbs the field only where it has gradients, this generates spread precisely at plume edges, where placement error is concentrated, while leaving the smooth background mostly intact.

The second component adds amplitude spread, in two independent forms. Persistent per-member multiplicative perturbation fields are applied to the dust and sea-salt concentrations. The first cycle perturbs the full domain, which doubles as the initial-condition amplitude spread, while subsequent cycles perturb only a tapered strip along the inflow boundary of the domain, emulating perturbed boundary conditions as fresh air enters the domain. Separately, each member is assigned a smooth random field applied as a linear per-cell weight on dust emission (Figure 4), held fixed throughout the run, so that members differ in the dust they emit within the domain as well as in the aerosol they import at the boundaries. The methodology used to generate the smooth fields is described in Tsikerdekis et al. 2021[2].

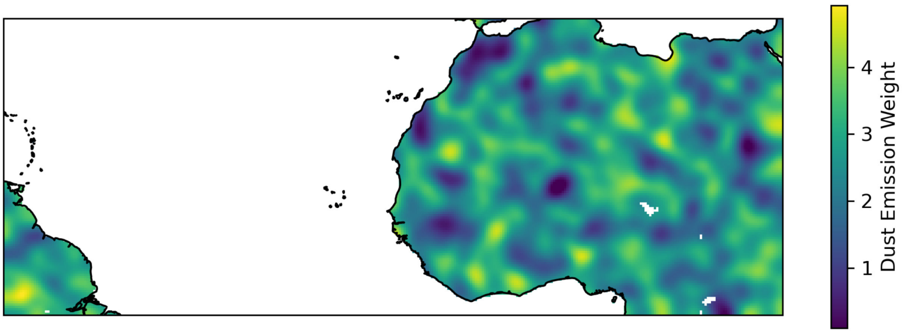

Figure 4: An indicative realisation of the emission perturbation field. Each model grid cell is assigned a coefficient that is applied multiplicatively to the emission flux.

The concentration perturbation fields are held fixed across cycles rather than redrawn, because boundary-condition error is time-correlated and reusing the fields gives each member a stable identity that the filter can learn over the cycling. The same realised perturbation fields, both the concentration fields and the emission weights, were generated once and shared across all three configurations, so that the control and the two assimilation runs carry an identical prior and differ only through the assimilation itself. Together these components cover the location and magnitude of the dust the model carries, both what it imports at the boundaries and what it emits within the domain, and the resulting free-running ensemble sustains a substantial spread throughout the experiment rather than collapsing toward a single trajectory.

L2A Extinction assimilation

Assimilating the Aeolus L2A extinction product produces a coherent and physically plausible adjustment to the dust field. Comparing the mean monthly AOD at 355 nm between the control and the L2A analysis (Figure 5) shows a difference of the order of 10% over the main Saharan outflow, consistent with the magnitude expected from theoretical considerations of the assimilated signal. The spatial structure of the difference tracks the dust plume, and the relative-difference field confirms that the largest adjustments occur where the mean dust load is highest, as expected for an observation type that constrains the aerosol directly. At the level of the individual overpass, the analysis reduces the extinction RMSE against the assimilated observations (Figure 6), confirming that the filter is drawing the model state toward the observations as intended.

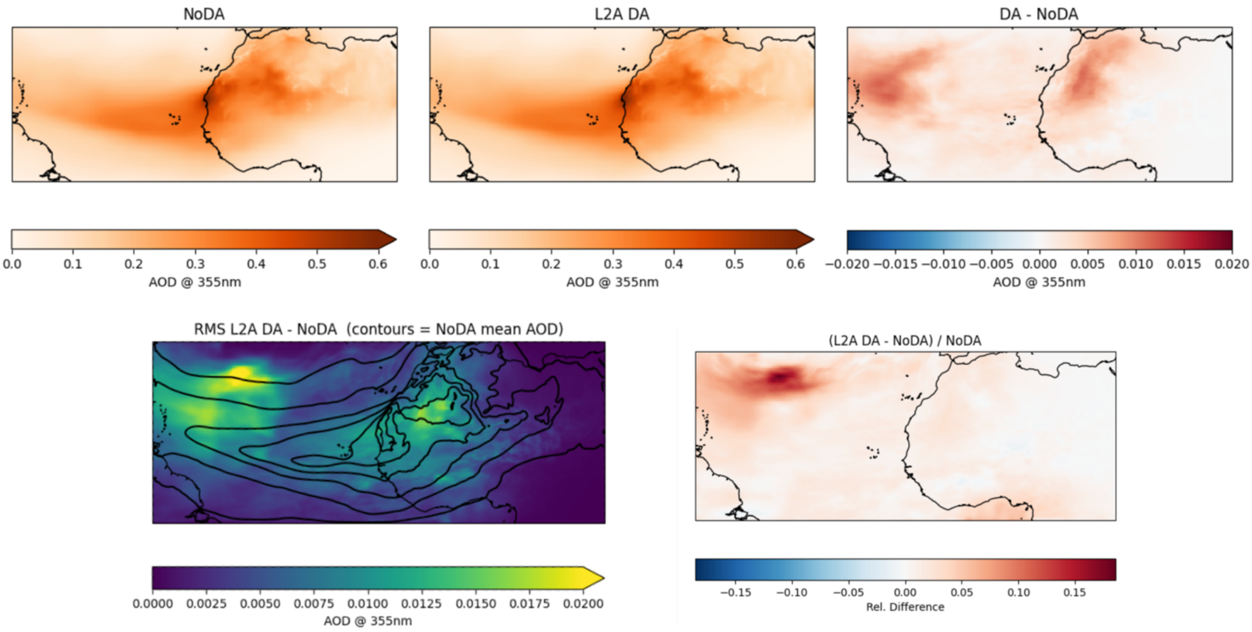

Figure 5: Top row shows the mean 355nm AOD for the control experiment (NoDA), the experiment with L2A assimilation (L2A) and their difference. Bottom row shows the root mean square difference between the two experiments (left panel) and the relative difference (right panel).

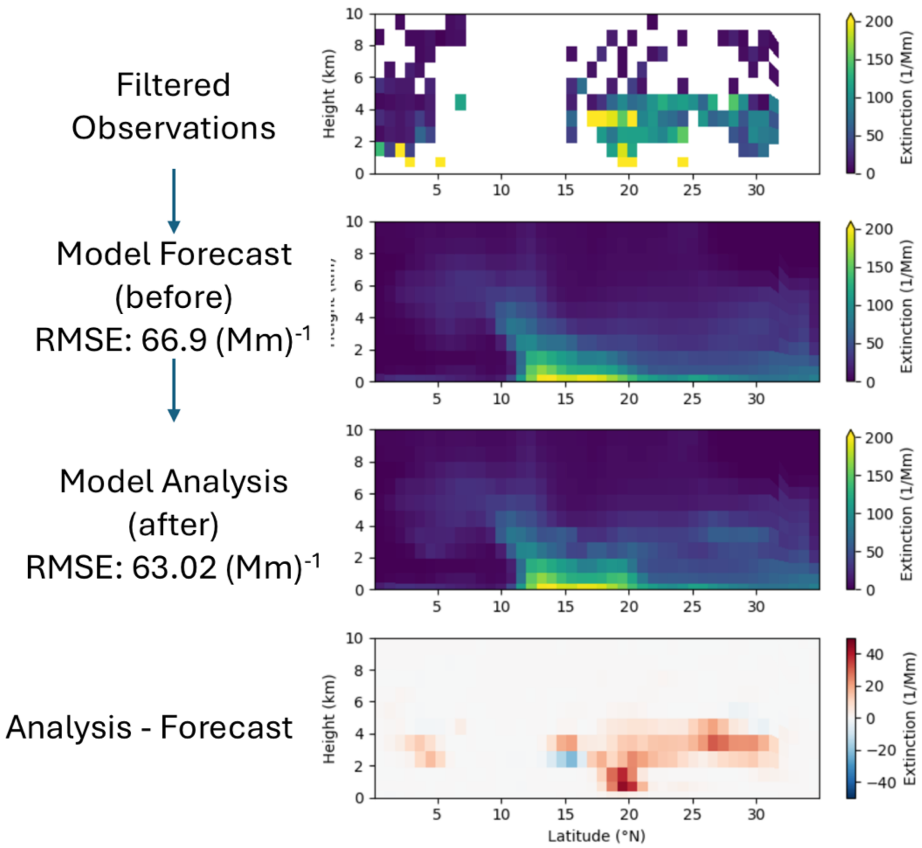

Figure 6: Assimilation of the overpass shown in Figure 3. Top row shows the observations used in the assimilation, second row shows the model forecast (or prior), and third row shows the model analysis (or posterior). Final row shows the difference between the analysis and forecast.

The magnitude of this impact is modest and the diagnostics explain why. Figure 7 compares the ensemble background spread with the assumed observation error as a function of altitude, together with the resulting per-observation gain. Throughout most of the column the ensemble is underdispersed relative to the observation error, so the implied Kalman gain is small. With a spread-to-observation-error ratio of the order of $\sigma_B/\sigma_o \approx 0.1$ and an aggregate gain of $K \approx 0.02$, each observation is permitted to move the analysis only slightly. The filter is operating close to its information limit, extracting the small correction that its assumed error budget allows rather than being throttled by any implementation deficiency. The sample-count panel further shows that observational coverage is sparse relative to the dust lifecycle, so that even this small per-observation increment is applied intermittently in space and time.

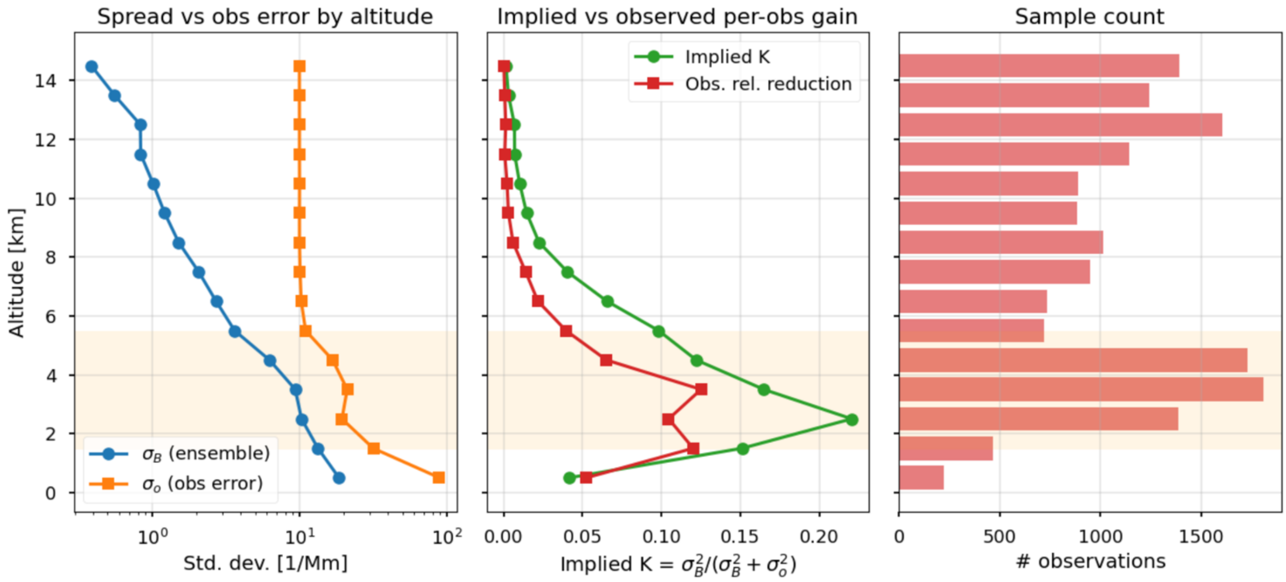

Figure 7: Comparison of ensemble spread and observation error for different altitudes, alongside kalman gain estimates and observation counts. The shaded area between 2 and 5.75km indicates the Saharan Air Layer, where most of the transported dust mass lives.

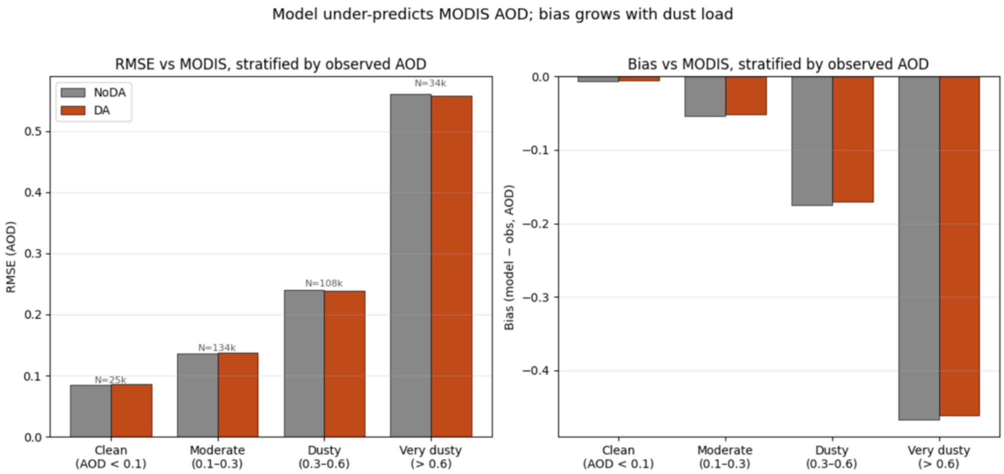

Figure 8: Root mean square error and bias of the two ensembles (control and L2A assimilation) against MODIS Deep Blue AOD observations for 4 different dust regimes.

A more fundamental limitation is that the model carries a large systematic background bias that assimilation of this kind cannot remove. Evaluated against MODIS AOD and stratified by observed dust load (Figure 8), the model exhibits a persistent negative bias that grows with dust load, from roughly -0.05 in moderately dusty conditions to -0.45 in the dustiest, with a corresponding growth in RMSE. An ensemble Kalman filter corrects the flow-dependent, random component of the error, but it is structurally unable to remove a systematic bias of this kind. The analysis is pulled toward the observations only within the span of the ensemble, and a bias shared by all members lies outside that span. The cloud screening compounds the problem, since it preferentially removes observations within the Saharan Air Layer, exactly the high-load regime where the bias is largest and where the observations would be most valuable. The extinction assimilation therefore behaves correctly as a filter, but its reach is bounded by three structural factors: the modest gain permitted by the ensemble spread, the sparse and cloud-screened coverage, and a systematic model bias.

L2B HLOS winds assimilation

Assimilating the Aeolus L2B HLOS wind product has a meaningful but small effect on the wind field itself. Figure 9 shows the ensemble background spread against the assumed observation error and the resulting per-observation gain, as a function of altitude, for the HLOS winds. In contrast to the extinction case, the implied gain is appreciable through much of the troposphere. The observations are informative and the analysis moves the wind field toward them across a broad vertical range. The impact on the winds is therefore not limited by information content and error budget in the way the extinction impact is.

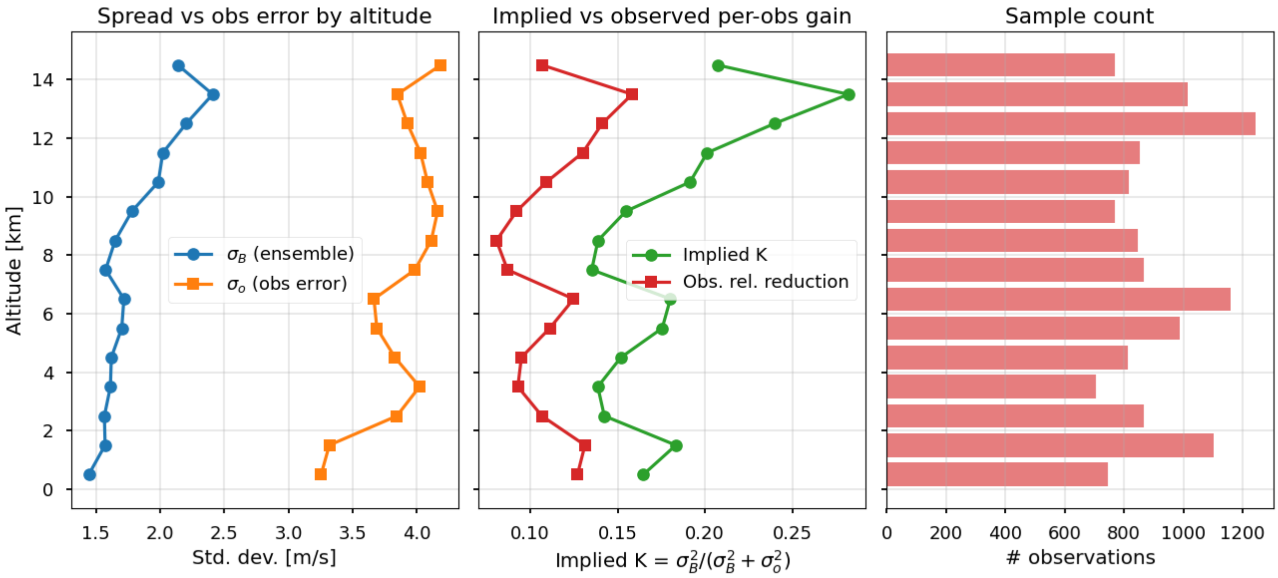

Figure 9: Comparison of ensemble spread and observation error for different altitudes, alongside kalman gain estimates and observation counts.

The effect on the dust field, however, is indirect. The L2B product constrains winds, not aerosol, so it can alter dust only through the transport that the corrected winds drive. Comparing the mean monthly AOD between the control and the L2B analysis (Figure 10) shows a difference that is spatially diffuse and smaller than the direct L2A adjustment, and, unlike the extinction case, not concentrated on the densest part of the plume. The relative-difference field is patchy rather than plume-following, consistent with a signal that propagates into the dust field through modified advection rather than through a direct correction of the aerosol amount. The resulting AOD change reflects redistribution more than adjustment of the total load, which is an expected result.

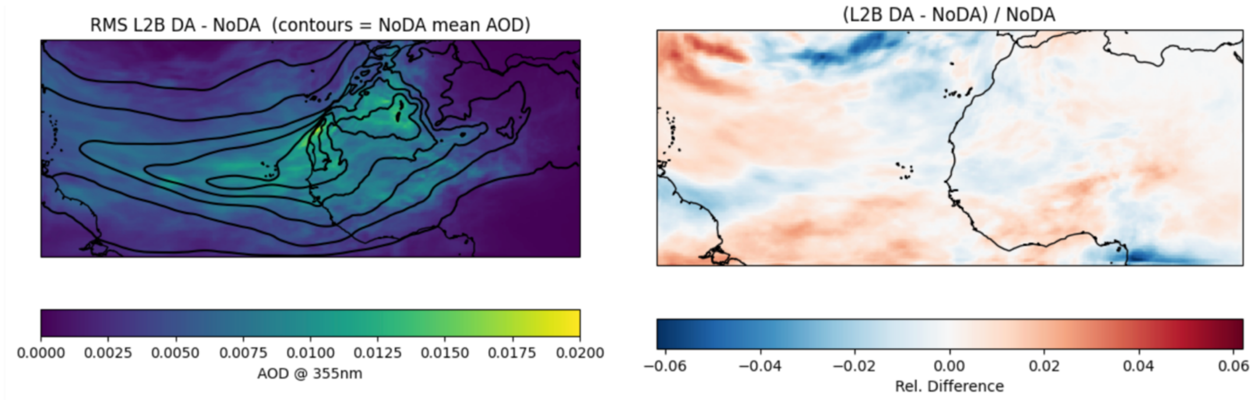

Figure 10: Root mean square (left) and relative (right) difference between the L2B assimilation and control ensembles.

Several factors keep this indirect impact small. First, the ensemble is underdispersed in HLOS observation space given the assigned observation error, which reduces the gain the filter is permitted even where the winds are informative. Second, the pathway is inherently lagged. Wind corrections reach the dust field only through transport and emission, so there is a latency between the analysis and any visible change in the aerosol, and a single cycle's increment has limited time to express itself before the next cycle. Longer experiments may therefore be needed to accumulate the effect. Third, dust emission appears to follow wind patterns that are largely unchanged between the experiments, so the surface source remains effectively uncoupled from the assimilation. Shifting the emission would require wind corrections large enough to alter the meteorological regimes that drive it, which the present increments do not reach. We are investigating richer expressions of the dynamical ensemble spread, such as stochastic perturbed parametrisation tendencies and spatially correlated perturbations, to relax the first of these constraints, while being careful not to degrade the forecast in the process.

Complementarity of the two products

Taken together, the two experiments show that extinction and wind assimilation act on different aspects of the dust problem. Figure 11 places the two impacts side by side, mapping the RMS difference between each analysis and the control against the mean dust distribution. The extinction impact is concentrated on the dense core of the plume, where the aerosol load is highest and the observations most directly constrain it, whereas the wind impact is displaced toward the plume margins and the transport pathways, where redistribution by the corrected winds is felt. The two patterns are differently distributed, a direct visual expression of the mechanistic difference established in the preceding sections. The L2A product corrects the aerosol amount where the dust already is, while the L2B product rearranges the dust through the flow that carries it.

This separation is what makes the two products complementary rather than redundant. Each addresses a different source of uncertainty in the modelled dust field, the aerosol state on the one hand and the transport that shapes it on the other, and neither substitutes for the other. Their benefits should also be broadly additive. Because they adjust the dust field in different places and through different mechanisms, assimilating both together would be expected to constrain the dust field more completely than either alone. The information content of a joint wind-and-aerosol lidar dataset is therefore greater than the sum suggested by either product in isolation, which is the central motivation for continued development of atmospheric lidar assimilation.

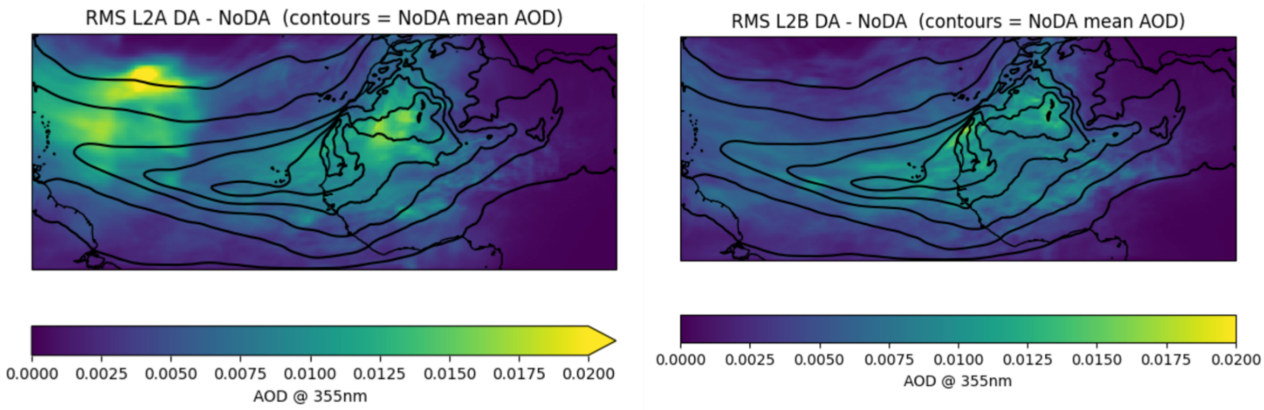

Figure 11: Root mean square difference between the assimilation experiment and the control ensemble for both products (L2A left, L2B right).

Acknowledgments

The computational resources of this project supported work funded under the ESA L2A+ project (4000139424/22/I-NS).

References

1. Feng, C. & Pu, Z. The impacts of assimilating Aeolus horizontal line-of-sight winds on numerical predictions of Hurricane Ida (2021) and a mesoscale convective system over the Atlantic Ocean. *Atmospheric Meas. Tech.* **16**, 2691–2708 (2023).
2. Tsikerdekis, A., Schutgens, N. A. J. & Hasekamp, O. P. Assimilating aerosol optical properties related to size and absorption from POLDER/PARASOL with an ensemble data assimilation system. *Atmospheric Chem. Phys.* **21**, 2637–2674 (2021).

List of publications/reports from the project with complete references

Work based on this project was presented in the following conferences:

- Georgiou T., Gialitaki A., Drakaki E., Tsikerdekis A., Tsekeri A., Marinou E., Melas D., Amiridis V.: Impact of combined wind and aerosol product assimilation, AEOLUS Science and CalVal Conference 2026, Lipari, Italy, 13-17 April 2026.
- Georgiou, T., Rizos, K., Tsikerdekis, A., Proestakis, E., Gkikas, A., Baars, H., Floutsi, A. A., Drakaki, E., Kampouri, A., Marinou, E., Donovan, D., Benedetti, A., McLean, W., Retscher, C., Melas, D., & Amiridis, V. (2023). Utilizing AEOLUS to Improve Dust Transport Modelling. Environmental Sciences Proceedings, 26(1), 193. https://doi.org/10.3390/environsciproc2023026193
- Alexandra Tsekeri, Anna Gialitaki, Matthew O'Callaghan, Thanasis Georgiou, Josef Gasteiger, et al.. Reproduce the backscatter of dust using realistic dust shapes. The 21th Electromagnetic and Light Scattering Conference, University of Messina, Jun 2025, Milazzo, Italy. pp.29 (hal-05142651)

- Georgiou, T., Tsikerdekis, A., Rizos, K., Proestakis, E., Gkikas, A., Drakaki, E., Kampouri, A., Baars, H., Floutsi, A. A., Marinou, E., Benedetti, A., McLean, W., Retscher, C., Melas, D., and Amiridis, V.: Using AEOLUS Aerosol Assimilation to pave the way for EarthCARE, EGU General Assembly 2024, Vienna, Austria, 14–19 Apr 2024, EGU24-10363, https://doi.org/10.5194/egusphere-egu24-10363, 2024.
- Georgiou, T., Proestakis, E., Gkikas, A., Rizos, K., Drakaki, E., Kampouri, A., Tsikerdekis, A., Baars, H., Floutsi, A. A., Benedetti, A., and Amiridis, V.: Enhancing Aeolus L2A for depolarizing targets and impact on aerosol research and NWP, EGU General Assembly 2023, Vienna, Austria, 23–28 Apr 2023, EGU23-17110, https://doi.org/10.5194/egusphere-egu23-17110, 2023

A journal publication based on the AEOLUS Science and CalVal Conference 2026 presentation is under preparation and will be submitted in 2027. In addition, some of the work references in this report also appears in project reports for the L2A+ project, available at the project website: https://l2a.space.noa.gr/

Future plans

(Please let us know of any imminent plans regarding a continuation of this research activity, in particular if they are linked to another/new EMI R&D Project.)

The developments carried out during this project, concerning the assimilation of atmospheric lidar profiles into a coupled composition model, are applicable not only to Aeolus but also to ground-based networks and to other satellite systems. The launch of EarthCARE, which carries the advanced ATLID high-spectral-resolution lidar, presents a strong opportunity to continue this line of work. ATLID improves on Aeolus in two respects that matter directly for the limitations identified here: it resolves the extinction and backscatter profiles at higher quality and with denser sampling and its depolarisation sensitivity provides information on particle shape that Aeolus does not and helps with feature classification.

That shape information bears on a source of uncertainty this project did not address, namely the optical operator that connects the model's dust mass to the observed extinction. The results reported here were obtained under the conventional assumption of spherical dust, but dust is markedly non-spherical, and the assumed optical properties determine how much mass a given extinction measurement implies. An error in those assumed properties is interpreted by the filter as an error in mass and corrected as such, so two analyses that agree in observation space can correspond to materially different dust burdens. Constraining the optical operator with shape-sensitive observations is therefore a natural next step toward analyses that are correct in mass and not only in the assimilated optical quantity.

A further aspect not examined here is how the constrained dust field feeds back on the rest of a coupled model, through its direct radiative effect and its role in cloud formation. Characterising that feedback is important if improved aerosol analyses are to translate into improved weather and air-quality forecasts, and it is a direction we intend to pursue.

This work is continuing under a follow-on project, also on the `spgramir` (2026) account, in which the lessons learned here are being applied to EarthCARE ATLID data. That project additionally tackles the optical-property uncertainty described above, assimilating extinction under updated non-spherical dust optical models so that the recovered dust mass, and not only the fitted extinction, is better constrained.